High-Resolution, >1 GHz NMR in Unstable Magnetic Fields

Y.-Y. Lin,[1] S. Ahn,[1] N. Murali,[2] W. Brey,[2] C. R. Bowers,[2,3] and W. S. Warren[1,*]
[1]*Department of Chemistry, Princeton University, Princeton, New Jersey 08544*
[2]*National High Magnetic Field Laboratory, Tallahassee, Florida 32306*
[3]*Chemistry Department, University of Florida, Gainesville, Florida 32611*
(Received 20 March 2000)

Resistive or hybrid magnets can achieve substantially higher fields than those available in superconducting magnets, but their spatial homogeneity and temporal stability are unacceptable for high-resolution NMR. We show that modern stabilization and shimming technology, combined with detection of intermolecular zero-quantum coherences (iZQCs), can remove almost all of the effects of inhomogeneity and drifts, while retaining chemical shift differences and J couplings. In a 25-T electromagnet (1 kHz/s drift, 3 kHz linewidth over 1 cm^3), iZQC detection removes >99% of the remaining inhomogeneity, to generate the first high-resolution liquid-state NMR spectra acquired at >1 GHz.

PACS numbers: 76.60.Lz, 07.57.Pt

A wide variety of NMR applications requires both high field and high resolution. The traditional advantages of high magnetic fields are improved sensitivity, enhanced resolution, and increased chemical-shift dispersion, among others [1]. In addition, even a moderately higher field than currently available has been predicted to significantly enhance the TROSY (transverse relaxation-optimized spectroscopy) line narrowing [2], and if this prediction is correct, the range of biomolecular sizes analyzable by NMR could be dramatically extended. Furthermore, there are certain problems that can be studied only at very high fields. Examples include field-induced phase transitions, highly correlated electron systems, spin ladders, powders with large quadrupole interactions, and molecular alignment due to anisotropic magnetic susceptibility [3]. With the advent of high upper-critical-field (H_{C2}) superconductors, the field strength of commercial NMR magnets has increased rapidly to the current value of 21 T (900 MHz ^{1}H Larmor frequency). It appears unlikely, however, that superconducting magnets beyond 23 T can be constructed in the foreseeable future unless new high H_{C2} materials become available [4].

Resistive (electromagnet) or resistive-superconducting hybrid magnets can achieve substantially higher static fields than those available in superconducting magnets; for example, the National High Magnetic Field Laboratory (NHMFL) has recently installed a 25-T electromagnet and a 45-T hybrid magnet. Unfortunately, the *spatial homogeneity* and *temporal stability* of the fields generated by these resistive or hybrid magnets are unacceptable for high-resolution experiments. For typical applications, high-resolution liquid-state NMR demands a spatial homogeneity on the order of 1 ppb/cm^3, a short-term temporal stability on the order of 1 ppb, and no detectable long-term drift. The requirements of a gigantic power supply (typically 10–40 MW) and a sophisticated cooling system, as well as other factors, make it highly unlikely that these issues will be resolved soon purely by advances in magnet engineering; the best current systems fall short of these specifications by a factor of 1000 or more. In this work, we show that these magnets can be effectively "homogenized" and "stabilized" by spin manipulations that exploit intermolecular zero-quantum coherences (iZQCs) to make possible high-resolution liquid-state NMR at very high fields.

High-resolution liquid-state NMR requires retention of chemical shift differences and J couplings. The spin echo sequence $\{(\pi/2) - \tau - \pi - \tau\}$ [5] or multiple-refocusing sequences such as the Carr-Purcell sequence $\{(\pi/2)_x - [\tau - (\pi)_x - \tau]_n\}$ [6] remove inhomogeneous broadening, but they also completely eliminate chemical shifts and J couplings if τ is much shorter than the reciprocal of the coupling constants. Reference deconvolution uses the experimental signal obtained for a known reference line to compensate for distortions imposed on the whole spectrum by the spectrometer [7], but a significant improvement in spectral linewidth exacts an unbearable penalty in signal-to-noise ratio and line shape, and the nonstationary line shape in a drifting magnet makes correction in complex sequences essentially impossible.

Another possible approach is to use multiple-quantum NMR, which explores the collective excitation and response of a group of coupled spins [8,9]. For example, total spin coherence transfer echo spectroscopy (TSCTES) takes advantage of the properties of the total spin coherence (the unique transition between the extreme eigenstates of a coupled spin system) to record multiple-quantum spectra free of inhomogeneous broadening yet sensitive to J couplings and chemical shift differences [8]. In addition, zero-quantum coherences (ZQCs), which connect pairs of states with the same number of spins-up (such as $\alpha\beta\beta$ and $\beta\alpha\beta$), are almost insensitive to field variations [9]. Unfortunately, uncoupled spins (singlets) cannot contribute to ZQC signals, the chemical shift information is not absolutely referenced to simplify spectral assignments, and calculating the intensities and phases of ZQCs for coupled spins requires a lengthy full-scale density matrix simulation of the pulse sequence with all spin parameters known *a priori*. More importantly, even though ZQCs or the TSCTES signals are immune to field inhomogeneity, they must be prepared from single-spin single-quantum coherences (SQCs, $\boldsymbol{I}_x$ and $\boldsymbol{I}_y$, where $\boldsymbol{I}$ is the spin operator) through J couplings between inequivalent spins [10], and must be detected by conversion into the same operators. Multiple-pulse refocusing, needed to remove the effects of field inhomogeneity or instability during the preparation and detection periods, will render this conversion ineffective. Hence conventional multiple-quantum experiments will not work for this application.

Our experiments use *intermolecular* ZQCs (iZQCs), which involve the mutual flip-flop of a solute-solvent spin pair [11–13]. For example, the pulse sequence $\{(\pi/2)_x - GT - t_1 - (\pi/4)_x - t_2 - (\pi)_x\}$, termed HOMOGENIZED for "homogeneity enhancement by intermolecular zero-quantum detection," was demonstrated in Ref. [13]. The distant dipolar field (DDF) provides the necessary through-space coupling between solute and solvent spins for the detection of iZQCs. In liquids, diffusion can only average away dipolar couplings between spins separated by distances much less than the mean diffusion path length on the NMR time scale (typically $\ll$10 μm). Because of the angular dependence of the secular dipolar Hamiltonian, the vector sum of the field contributions from distant spins is negligible for a uniformly magnetized, near-spherical sample. Spatial magnetization modulation created by free precession in a field gradient, however, can break the symmetry and reintroduce this dipolar effect. The surviving dipolar couplings for a distant spin pair are individually quite small ($\approx 10^{-11}$ rad/s), but the very large number of neighboring spins generates an easily observable effect ($\approx$10 rad/s). As long as the field is homogeneous over the separation of the solute-solvent spin pair (adjusted by the strength of one gradient pulse, typically 10–100 μm), the resulting iZQC spectra would be just the conventional SQC spectrum of the solute, shifted by the chemical shift of the solvent. Consequently, chemical shift differences and coupling information for the solute are retained, yet the effects of field inhomogeneity and instability are practically eliminated.

The underlying evolution of the density operator has been detailed elsewhere [12,14]. In summary, iZQCs stem from the multispin operators produced when the full equilibrium density operator without the high-temperature approximation is first excited by the $(\pi/2)_x$ pulse. The pulsed gradient GT then serves as a ZQC filter by dephasing out all other coherences. Let $\boldsymbol{I}$ and $\boldsymbol{S}$ denote the spin operators for the solvent and solute, respectively. During t_1 evolution, the solvent-solute ZQCs (terms such as $\boldsymbol{I}_{+i}\boldsymbol{S}_{-k}$) are modulated by the difference of the Larmor frequencies, while the solvent-solvent or solute-solute ZQCs (terms such as $\boldsymbol{I}_{+i}\boldsymbol{I}_{-j}$ and $\boldsymbol{S}_{+k}\boldsymbol{S}_{-l}$) will not be modulated at all. The $(\pi/4)_x$ pulse then transfers these ZQCs into two-spin SQCs such as $\boldsymbol{I}_{xi}\boldsymbol{I}_{zj}$, $\boldsymbol{I}_{xi}\boldsymbol{S}_{zk}$, and $\boldsymbol{S}_{xk}\boldsymbol{S}_{zl}$. During t_2 evolution, these terms will be rendered observable by the action of the DDF, which needs a time on the order of τ_d to appear [11–13]. In the absence of inhomogeneity or drift, the detected transverse magnetization M obeys

$$M(t_2) \propto J_1\left(\frac{t_2}{\sqrt{2}\tau_d}\right), \qquad \tau_d = (\gamma\mu_0 M_0)^{-1}, \qquad (1)$$

where J_1 is the Bessel function of the first kind, μ_0 is the magnetic permeability of a vacuum, and M_0 is the equilibrium magnetization at B_0. For a pure water sample at 300 K, τ_d is 37 ms at 25 T. iZQCs have also found applications in MRI contrast enhancement for tumor detection and functional imaging [15] and in probing intermolecular correlations at an adjustable separation dictated by the gradient strength [16].

For this application, iZQCs have one critical advantage over conventional ZQCs: they are detected using dipolar couplings, so their effects are not eliminated by echo pulse trains. They also produce a much simpler spectrum; solute-solvent iZQCs have the intensity and multiplet structure of the conventional spectrum in a homogeneous magnet.

It is not obvious that the HOMOGENIZED experiment [13] can be extended to a realistic high-field electromagnet, since two separated molecules are involved in an iZQC. We used NHMFL's Keck resistive magnet (25.0 T field, 1.06 GHz ^{1}H Larmor frequency). It has a modified Bitter design with a bore diameter of 52 mm, and consumes 13.8 MW at 38.8 kA. Deionized cooling water is circulated through the magnet at the rate of 4500 L/min with a temperature/pressure of 8.9 °C/2.9 MPa at inlet and 45.4 °C/1.2 MPa at outlet. A flux stabilizer (pickup and compensating coils axially parallel to B_0) partially compensates for the resulting temporal field instability. Under ideal operating conditions, Keck was designed to achieve 2-ppm/cm^3 spatial homogeneity after passive shimming and 1-ppm temporal stability during data acquisition. However, it is exceedingly difficult to calculate the expected current distribution and fluctuations with the accuracy needed to determine either short-term ($<$1 ms) field fluctuations or local field structure, and both of these effects could affect any NMR measurement. Hahn-echo experiments presented in Fig. 1(a)–1(c) show that pulse intervals $\ll$1 ms on the Keck magnet give stable spin echoes in both phase and amplitude. Longer pulse intervals in the 2–10 ms range (data $>$2 ms not shown) generate random phase fluctuations but do not result in significant amplitude/line shape changes. It may be inferred that field fluctuations have Fourier components concentrated below 1 KHz and homogeneity changes have negligible components distributed above 100 Hz. The multiple-echo CPMG sequence gives largely superimposable echoes [Fig. 1(d)], in good agreement with the studies of NMR phase noise in Bitter magnets [17]. Together these experiments imply that the micron-scale broadening contribution must be very small, since molecular diffusion

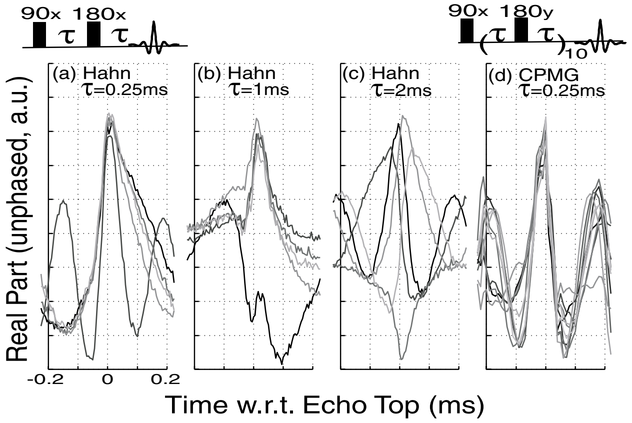

FIG. 1. Spin echo generated by (a)–(c) Hahn echo sequence (five superimposed) and (d) CPMG sequence (ten superimposed). Note that the echoes in (a) and (d) are superimposable at the peak.

would prevent a CPMG sequence from refocusing this component. This implies that the sequence in Ref. [13], which used a single echo in the detection period to compensate for static inhomogeneity, will not work, but that detection using a CPMG sequence (Fig. 2, inset) is feasible. Further improvement in pulse performance is achieved here through composite pulses, which replace a standard rectangular pulse with a carefully chosen combination of back-to-back or delayed rectangular pulses with phase shifts to cancel out each other's imperfections.

The 5-mm high-resolution probe with a shielded z-gradient assembly was custom fabricated by Doty Scientific, Inc. (Columbia, SC) for use with this specific magnet. The experimental effects of our composite CPMG-HOMOGENIZED sequence on a 1:1 water/acetone solution in a 5-mm NMR tube at 20 °C without spinning are demonstrated in Fig. 2(a). The iZQC spectrum exhibits the expected peaks at the precise frequency differences with correct phase alternation, in agreement with quantum-mechanical (density operator) and classical (modified Bloch equations) analysis [14]. The two peaks at $2\omega_{IS}^{ZQ}$ and $2\omega_{SI}^{ZQ}$ arise from higher-order solvent-solute ZQCs such as $\boldsymbol{I}_{+i}\boldsymbol{I}_{+j}\boldsymbol{S}_{-k}\boldsymbol{S}_{-l}$ and $\boldsymbol{I}_{-i}\boldsymbol{I}_{-j}\boldsymbol{S}_{+k}\boldsymbol{S}_{+l}$ [14]. These double-frequency peaks would not be observable in a more typical application, with very different solute/solvent concentrations. The validity of the experimental results is further confirmed through comprehensive numerical simulations based on modified Bloch equations and finite difference method [18], shown in Fig. 2(b), where all the effects of T_1, T_2 relaxations, diffusion, DDF, and field inhomogeneity and instability are included.

Figure 2 shows that the ≈3-KHz apparent linewidth in a normal single-shot spectrum (linewidth in F_2) is reduced to ≈30 Hz in F_1, limited by truncation effects. Data from this sample and the singlet peak from a 1:1 methyl ethyl ketone/water mixture (not shown) have been fitted by a matrix pencil method [19] to give a linewidth

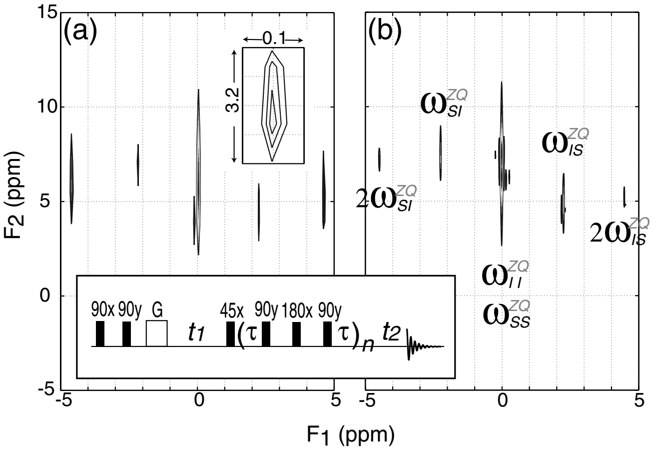

FIG. 2. (a) Experimental and (b) simulated intermolecular ZQC spectra by composite CPMG-HOMOGENIZED sequence, plotted at a contour level of 3 times of the noise standard deviation. The ω_{IS}^{ZQ} peak in (a) is magnified in the insert, plotted at the same contour level. Pulse sequence and simulation parameters: $\pi/2$ pulse length 15 μs, water $\sigma_I = 0$ ppm, acetone $\sigma_S = 2.2$ ppm, $\tau = 0.25$ ms, $n = 60$, $GT = 10$ gauss · ms/cm, $T_1 = 3.05$ s, $T_2 = 2.10$ s, and diffusion coefficient $D = 2 \times 10^{-5}$ cm^2/s. The simulation assumes a field inhomogeneity of 1 ppm/cm, field fluctuations modeled by Gaussian white noise with 0.5-ppm standard deviation and 1-KHz upper frequency limit, and a sample length of 0.9865 cm sampled by 400 spatial points on the z axis.

of 23 Hz (full width at half height); the (methyl-ethyl-ketone–water) multiplets are partially split by the J couplings, but not fully resolved ($J \approx 8$ Hz). This linewidth is limited by residual inhomogeneity over the correlation distance $d = \pi/\gamma GT$, which is 120 μm in these experiments. Stronger gradient pulses will reduce the linewidth further, until the correlation distance becomes comparable to the distance that molecules diffuse during the sequence. The ultimate limit is twice the homogeneous linewidth (since two spins are involved), which is less than 1 Hz in this sample.

The pulse sequence in Fig. 2 can be easily adapted for other experiments. As shown in Ref. [20], iZQCs which combine complex, multispin evolution on the solute molecule with solvent coherences can be detected; so can heteronuclear multiple-quantum coherences [21]. The TSCTES principle of using evolution of an unstructured peak (there, the highest-quantum coherence) to compensate inhomogeneity can be adapted to these experiments, since the single-quantum solvent evolution is also an unstructured peak. Replacing the composite pulses by amplitude- or phase-modulated shaped pulses [22] or self-compensated iterative pulses [23] will also be useful, to extend the uniformly excited bandwidth or help circumvent the artifacts of incomplete refocusing. A goal for future work is to verify predictions of significant resolution enhancement in large biomolecules through TROSY at very high field. At Keck's 1.06-GHz ^{1}H Larmor frequency, the destructive interference between dipolar and chemical-shift-anisotropy interactions within ^{15}N-^{1}H moieties is predicted to be nearly complete [2]. The inherently high signal-to-noise ratio at very high field may eventually allow ZQC spectra to be directly recorded without time-consuming two-dimensional data acquisition [24]. Further implementation of this method on the much more powerful hybrid magnets should be straightforward, since the mutual inductance between the resistive insert and the stable superconducting outsert will give greater stability than a resistive magnet alone [4].

In summary, we have demonstrated *the first ever high-resolution NMR spectrum taken at* >1 *GHz*. The effects of spatial inhomogeneity and temporal instability of the magnetic field on the spectra are nearly eliminated, thereby achieving a resolution enhancement of ≈ 100. Scalar coupling effects during t_1 are preserved by this sequence. The approach of complementing advancements in magnet technology with such methodological innovation in spin engineering provides unique and critical advantages. For these very-high-field magnets, these experiments give previously inaccessible information relevant to ultimate improvements in high-field magnet design, and the added NMR functionality expands their applicability well beyond the original envisioned purpose. For the high-resolution NMR community, the approach gives access to substantially higher fields than were previously thought possible, thus opening new frontiers.

This work was supported by the NIH under Grant No. GM35253 and the NHMFL. We wish to explicitly thank Dr. Jack Crow for his support.

---

*To whom correspondence should be addressed.

[1] T. Meersmann, M. Schwager, V. Varma, and G. Bodenhausen, J. Magn. Reson. A **119**, 275 (1996).
[2] K. Pervushin, R. Riek, G. Wider, and K. Wuthrich, Proc. Natl. Acad. Sci. U.S.A. **94**, 12 366 (1997).
[3] J. S. Brooks, J. E. Crow, and W. G. Moulton, J. Phys. Chem. Solids **59**, 569 (1997).
[4] P. L. Kuhns, A. Kleinhammes, W. G. Moulton, and N. S. Sullivan, J. Magn. Reson. A **115**, 270 (1995).
[5] E. L. Hahn, Phys. Rev. **80**, 580 (1950).
[6] H. Y. Carr and E. M. Purcell, Phys. Rev. **94**, 630 (1954).
[7] G. A. Morris, H. Barjat, and T. J. Horne, Prog. NMR Spectrosc. **31**, 197 (1997).
[8] M. Munowitz and A. Pines, Science **233**, 525 (1986).
[9] R. R. Ernst, G. Bodenhausen, and A. Wokaun, *Principles of Nuclear Magnetic Resonance in One and Two Dimensions* (Clarendon, Oxford, 1987).
[10] A. Abragam, *Principles of Nuclear Magnetism* (Clarendon, Oxford, 1961).
[11] W. S. Warren, W. Richter, A. H. Andreotti, and B. T. Farmer II, Science **262**, 2005 (1993).
[12] S. Lee, W. Richter, S. Vathyam, and W. S. Warren, J. Chem. Phys. **105**, 874 (1996).
[13] S. Vathyam, S. Lee, and W. S. Warren, Science **272**, 92 (1996).
[14] S. Ahn, N. Lisitza, and W. S. Warren, J. Magn. Reson. **133**, 266 (1998).
[15] W. S. Warren *et al.,* Science **281**, 247 (1998).
[16] W. Richter, S. Lee, W. S. Warren, and Q. He, Science **267**, 654 (1995).
[17] E. Sigmund *et al., NHMFL 1999 Annu. Res. Rev.* 187 (2000).
[18] T. Enss, S. Ahn, and W. S. Warren, Chem. Phys. Lett. **305**, 101 (1999).
[19] Y.-Y. Lin, P. Hodgkinson, M. Ernst, and A. Pines, J. Magn. Reson. A **128**, 30 (1997).
[20] S. Ahn, S. Lee, and W. S. Warren, Mol. Phys. **95**, 769 (1998).
[21] P. Bachiller, S. Ahn, and W. S. Warren, J. Magn. Reson. A **122**, 94 (1996).
[22] W. S. Warren and M. S. Silver, in *Adv. Magn. Reson.,* edited by J. S. Waugh (Academic Press, San Diego, 1988), Vol. 12.
[23] R. Tycko, A. Pines, and J. Guckenheimer, J. Chem. Phys. **83**, 2775 (1985).
[24] A. Bax, T. Mehlkopf, J. Smidt, and R. Freeman, J. Magn. Reson. **41**, 502 (1980).